Hindawi
Mobile Information Systems
Volume 2021, Article ID 9032769, 8 pages
https://doi.org/10.1155/2021/9032769

Research Article

Analysis of the Movement Characteristics of the Pump Valve of the Mine Emulsion Pump Based on the Internet of Things and Cellular Automata

Ran Li,[1,2] Dalong Wang,[3] Wenshu Wei,[2] and Shoubin Li[4]

[1]*Graduate School, CCRI, Beijing 100013, China*
[2]*Beijing Tianma Electronic-Hydraulic Control System Company Ltd., Beijing 100013, China*
[3]*School of Mechanical Electronic & Information Engineering, China University of Mining and Technology Beijing, Beijing 100083, China*
[4]*Research Institute of Mine Big Data, CCRI, Beijing 100013, China*

Correspondence should be addressed to Dalong Wang; wangdl@student.cumtb.edu.cn

Received 24 June 2021; Revised 15 July 2021; Accepted 28 July 2021; Published 3 August 2021

Academic Editor: Fazlullah Khan

Studying the movement characteristics of the coalmine emulsion pump valve is of great significance for optimizing the dynamic response characteristics of the pump valve, reducing the hysteresis effect, and improving the volumetric efficiency. This article combines the Internet of Things (IoT) and cellular automata techniques to investigate the movement characteristics of the valve of the emulsion pump. Based on Adolf's exact differential equation and Runge–Kutta iterative method, the movement displacement and movement of the pump valve spool speed curve are computed using Scilab software. We employ cellular automata and AMESim to establish the hydraulic system model of emulsion pump and analyze the movement characteristics of pump valve movement displacement, speed, stability, and closing hysteresis through simulation. Finally, the IoT techniques and a test device are used to evaluate the movement displacement of the pump valve. The experimental results verify the feasibility of using the proposed method to study the pump valve motion characteristics, greatly reduce the cost of testing and parameterized design, and contribute to the development of highly reliable and efficient emulsion pump valves.

1. Introduction

The coalmine emulsion pump is a typical reciprocating plunger pump. It is the power source of the fully mechanized mining hydraulic systems. It delivers high-pressure media to the fully mechanized mining hydraulic support and is an important source for continuous and efficient mining of the entire working face [1, 2]. The pump valve of the emulsion pump is an important flow distribution mechanism, which can provide the delivery of the emulsion. Due to the compressibility of the emulsion medium, the valve distribution response of the emulsion pump has a certain hysteresis [3]. The hysteresis in the process of pump valve distribution is the main reason that affects the volumetric efficiency of the emulsion pump. Therefore, studying the movement characteristics of the pump valve of the emulsion pump is of great significance for optimizing the dynamic response characteristics of the pump valve, reducing the hysteresis effect, and improving the volumetric efficiency [4, 5].

Gustav Adolph Mayer (U-Adolph) [6] demonstrated the second-order nonlinear ordinary differential equation describing the dynamic characteristics of the pump valve under the assumption of liquid incompressibility. Combined with the differential equations of Adolf's pump valve motion, several works have carried out research on the motion law of the reciprocating plunger pump valve. Omichi et al. [7] studied the influence of the Widmanstätten effect of the pump valve movement on the continuous flow conditions of the liquid in the pump barrel and established a simulation model of the pump valve movement law by using the

numerical integration method. Junfeng et al. [8] developed an experimental system for evaluating valve disc's motion parameters to directly obtain the valve disc motion acceleration, velocity, and displacement under real conditions. The testing results were compared with the calculation results obtained according to U. Adolph Theory and Approximation Theory. The authors in [9] investigated the dynamic features of the cartridge pilot relief valve by power bond graph and AMESim simulation software and reported the impact of main structural parameters on its dynamic performance. Lei and Wu examined the stability and fast responsiveness of the relief valve and improved the structure of the relief valve through simulation [10]. Dasgupta and Watton employed the bond graph approach to investigate the dynamic characteristics of the valve and obtained the influence of damper hole, spring, and other structures on the response of the relief valve system [11]. Sang and Kang [12] studied the spool damper hole of the emulsion pump valve. Fluent was used to simulate the flow field near the damper hole with different diameters. Using the damper hole, the structure of the relief valve was improved. Vallet et al. [13] used the bond graph method to study the dynamic characteristics of the pilot relief valve. Taking into account the static hydrodynamic force and hydraulic compressibility of the valve core, the impact of body structural factors of the valve on response time was simulated. The effect of the change in the diameter of the damper hole and the half-cone angle of the main spool on the peak time and the adjustment time of the emulsion pump valve is obtained. Hao et al. [14] used AMESim simulation software to investigate the opening characteristics, hysteresis response, closing shock, and other characteristics of different types of emulsion pump valves. The authors in [15] combined the simulation results of the dynamic characteristics of AMESim, using software to optimize the spool structure, reducing the impact stress when the spool is closed. Xiu and Yajun [16] completed a simulation of the hydraulic relief valve and established the AMESim model of the valve. They examined the effect of pilot valve lead clearance, valve core mass, sensitive chamber volume, damping hole diameter, spring stiffness, and other parameters on system performance. Yongjun et al. [17] developed a hydraulic back pressure valve. The effects of the front volume of the main throttle, the volume of the main spring chamber, the size of the slim hole of the damper plug, and the main throttle on the performance of the damper were discovered using simulation. Some scholars have proposed the mathematical model of the emulsion pump valve and linearized the differential equation to get the transfer function model of the valve. The dynamic performance of the emulsion pump valve and the influence of structural parameters on the performance of the valve were simulated and analyzed using Matlab/Simulink and other simulation methods [18–21]. Tian et al. [15] simulated the fluid supply line of the emulsion pump station using AMESim software, and the pressure loss model was simulated and analyzed. The power matching control technology was introduced into the pump station control system to judge the power demand of hydraulic support and optimize the output of the emulsion pump station.

As the only key equipment that provides power to the hydraulic support, the emulsion pump valve is the reliable operation of the hydraulic support and the safe operation of the underground [16]. Therefore, the performance of the emulsion pump is very important. Studying the movement characteristics of the pump valve of the emulsion pump is of great significance for optimizing the dynamic response characteristics of the pump valve, reducing the hysteresis effect, and improving the volumetric efficiency. This article combines the IoT and cellular automata to analyze the movement characteristics of the pump valve of the mine emulsion pump. It is expected that the copper drum will therefore optimize the performance and structural parameters of the emulsion pump, which can have a definite guiding role in the design of emulsion products.

The rest of the paper is organized as follows. Section 2 provides an overview of the related technologies. In Section 3, the cellular automata and Adolf differential equations are discussed. Section 4 illustrates the simulation results, and finally, Section 5 concludes the manuscript.

2. Overview of Related Technologies

2.1. Emulsion Pump Valve Distribution Principle. The coalmine emulsion pump is usually driven by a motor and is reduced by a first-stage gear to drive the crankshaft to rotate, and then the connecting rod and the crosshead drive the plunger to reciprocate [17, 18]. The rightward movement of the plunger is the discharge stroke, the leftward movement is the suction stroke, and the crankshaft is rotated one time. The discharge valve and the suction valve are opened and closed each time. Figure 1 shows the data processing structure of the emulsion pump.

During this process, the working fluid passes through the suction valve and the discharge valve, and the liquid is delivered [18, 19]. The emulsion pump depends on the rotation of the crankshaft to drive the plunger to reciprocate so that the volume of the working chamber changes periodically to complete the suction and discharge process of the emulsion pump [20, 21]. The suction and discharge process consists of the opening and closing of the pump valve. If the suction and discharge valves and the plunger have good sealing performance, there is no leakage during the movement of the spool [22, 23]. Figure 2 shows the working mechanism of the emulsion pump.

Under normal circumstances, both sides of the spool of the suction valve are filled with liquid medium. When the plunger moves away from the hydraulic end, the pressure in the cavity is rapidly decreased to form a low-pressure vacuum [24]. Currently, the pressure outside the spool is lower than the pressure in the cavity, resulting in pressure change. When the pressure of the working chamber is reduced to a certain value, the external liquid pressure overcomes the spring force of the valve core and the weight to push the suction valve open [25]. At this time, the medium liquid enters the plunger chamber. In the process of the plunger turning to the right, as the plunger continues to move to the right, the pressure in the working chamber increases [26]. When the pressure in the working chamber

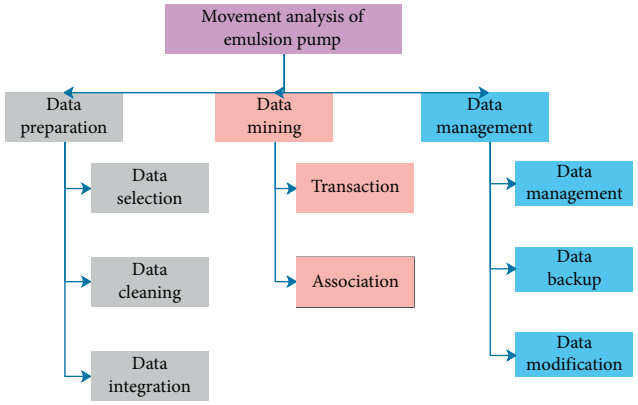

Figure 1: Data processing structure of emulsion pump.

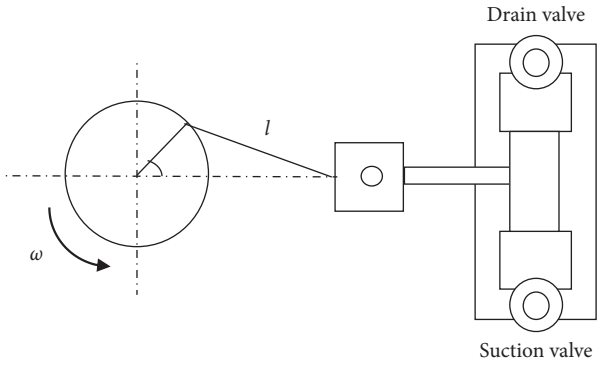

Figure 2: Working principle of the emulsion pump.

closes the suction valve core, the liquid pressure in the working chamber is greater than the discharge pressure. The spring drain valve core of the liquid valve core is opened, and the emulsion is discharged from the drain valve.

2.2. Internet of Things Technology. The Internet of Things (IoT) is a system of interconnected computing devices, mechanical and digital machines, objects, and people that are provided with distinct identifiers and the ability to transfer data over a network without requiring human-to-human or human-to-computer interaction. In recent years, with the advent of various sensor technologies and the development of cloud computing technology, the IoT has begun to become the focus of social attention and has gradually begun to develop [27]. Sensors could be motion sensors, air quality sensors, temperature sensors, moisture sensors, and light sensors. These sensors, along with a connection, allow us to automatically collect information from the environment, which, in turn, allows us to make more intelligent decisions. Recently, service-oriented architecture and cloud computing technology have been greatly developed. Many manufacturers combine IoT platforms with clouds, design and implement IoT platforms with service-oriented thinking, and encapsulate various underlying devices into services that are connected to the platform in a unified way, and devices are unified as services for management so that all devices have a unified way of access and expression in the platform. At the same time, devices open platform regulations [28, 29].

To reduce costs, existing IoT application scenarios deploy network facility nodes in fixed locations that are easy to deploy and manage, and the number is limited [30, 31]. Under this fixed-topology network deployment method, some areas such as construction sites, fire/earthquake sites, and large-scale and assembly sites are damaged due to the complex construction environment or accidentally damaged, and the coverage performance is greatly reduced or even become coverage blind spots. Therefore, it is necessary to increase the flexibility of the network in the above-mentioned area and flexibly supplement and change the location of network nodes [32, 33].

3. Analysis of Pump Valve's Movement Characteristics

3.1. Cellular Automata. A cellular automaton is a lattice of cells where the behavior of each cell is determined by the behavior of its neighboring cells as well as the automata rule. It can simulate the spatiotemporal evolution process of complex systems. According to spatial levels, cellular automata are divided into one-dimension, two-dimension, and high-dimension models. The simplest type of cellular automata is a binary, nearest neighbor, one-dimensional automaton. Such types of automata are also called "elementary cellular automata." Cellular automata are composed of four parts: cell, cell space, neighbors, and transformation rules. The definitions of the four parts are different due to different models. In general, the cellular automata can be regarded as a transformation function defined in a specific cell space [20].

Because of the single state set and simple rules, the emulsion pump depends on the rotation of the crankshaft to drive the plunger to reciprocate so that the volume of the working chamber changes periodically to complete the suction and discharge process of the emulsion pump. Experts and scholars have studied it deeply, and it is the basis of all cellular automata models.

$$\frac{d\vartheta}{dt} = \omega_z, \qquad \alpha = \vartheta - \theta. \tag{1}$$

Rules are the core of the cellular automata model. The cell and cell space only represent the static components of the system, and the characteristics of cellular automata are discrete and dynamic.

$$\frac{dx}{dt} = V\cos\theta, \qquad \frac{dy}{dt} = V\sin\theta. \tag{2}$$

To introduce dynamics, we need to add the corresponding cell transformation rules [21]. The schematic diagram of cell data processing is shown in Figure 3.

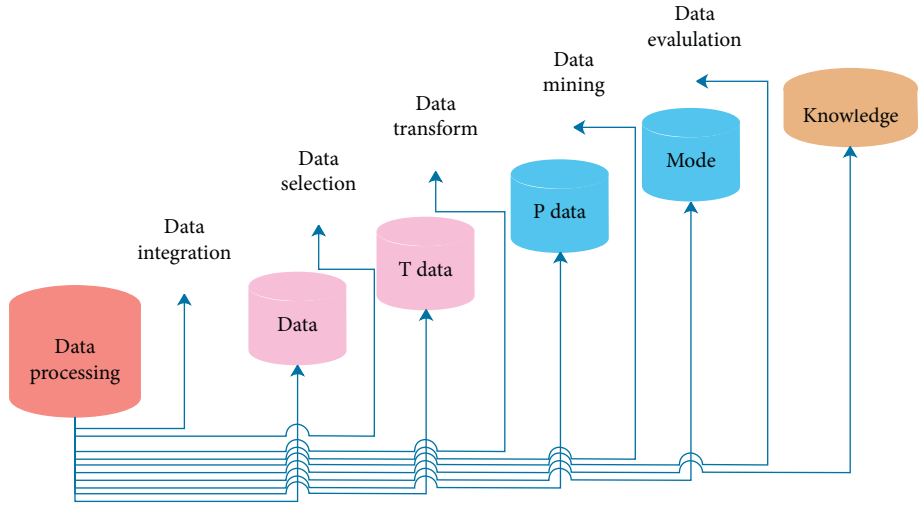

Figure 3: Schematic diagram of cell data processing.

The main steps included are data integration, data selection, transformation, mining, and evaluation.

The transformation rule can be given represented as mathematics and physical equations and generally depends on specific conditions. The function can be expressed as follows:

$$J_z \frac{d\omega_z}{dt} + \left(J_y - J_x\right)\omega_y\omega_x + J_{xy}\left(\omega_y^2 - \omega_x^2\right) = M_z. \tag{3}$$

The cell adjacent to the central cell in space is called its neighbor, and the area composed of all neighbors is called the cell neighborhood.

$$\begin{aligned} &\delta_z = f\left(e_1\right), \\ &q_7 \equiv \theta_{10} = a \tan 2\left(-s_5 n_{ex} + c_5 n_{ey}, s_5 a_{ex} - c_5 a_{ey}\right). \end{aligned} \tag{4}$$

Owing to the complex characteristics of the emulsion pump, it is assumed that the neighbors of a cell are other cells connected to it at the network level, and the adjacency matrix A is used to represent the neighbor relationship between these neighbor cells.

$$\begin{aligned} C_i &= -\frac{1}{2}\eta M^{-1}1, \\ \mathrm{Arg}C_i &= \frac{\sum_{i=1}^{n}\sum_{j=1\wedge\neq j}^{n} CC\left(S_i, S_j\right)}{n * (n-1)}. \end{aligned} \tag{5}$$

To determine the transmission trend and the impact scale under the node cascade failure, we compute

$$\mathrm{Arg}CC\left(C_i, C_j\right) = \frac{\sum_{i=1}^{m}\sum_{j=1\wedge\neq j}^{n} CC\left(S_i, S_j\right)}{m * n}, \tag{6}$$

$$f = \sum_{j=1}^{4} f_j w_j, \tag{7}$$

$$F_j = \frac{1}{\left(1 + \sum_{j=1}^{4} f_j w_j\right)}. \tag{8}$$

A cellular automaton (CA) is an open, flexible, and discrete dynamic model that holds enormous potentials in modeling complex systems, despite the simplicity of the model itself. In summary, cellular automata have a long research history and are widely and maturely applied in various fields. It has formed a relatively complete theoretical system. Only simple transformation rules of CA can be used to realize the complex systems that are difficult to calculate. Simulation evolution: owing to its impressive power, intuitiveness, and relative simplicity, the CA approach has great potential for use as a tool in emulsion pump valves. Therefore, it is feasible to use cellular automata to study the key parameters of emulsion pumps [21, 22].

3.2. Adolf's Exact Differential Equation. Adolf's exact differential equation model has singularities with the opening and closing phases of the valve. Therefore, the Runge–Kutta method is used to iteratively solve the second-order nonlinear ordinary differential equations. Runge–Kutta method is an effective and mostly used method for computing the initial-value problems of differential equations. It can be used to construct high-order accurate numerical methods. Based on the Runge–Kutta method, a simulation model describing the movement of the pump valve is developed, and a simulation program describing the movement of the pump valve was compiled using Scilab simulation software [34]. The second-order nonlinear ordinary differential equation describing the dynamic characteristics of the pump valve deduced by U-Adolph is shown as follows:

$$T^2h^2h'' + h^3 + Ah^2 - \varepsilon Bf^2 + \varepsilon Cfh' - \varepsilon\, Dh'^2 = 0, \tag{9}$$

where $T^2 = m/c$, $A = ((G + F_S')/c)$, $B = (\varphi\xi\rho A^2 A_v r^2\omega^2/2cl_v^2\sin^2\alpha)$, $C = (\varphi\xi\rho A A_v^2 r\omega/cl_v^2\sin^2\alpha)$, and $D = (\varphi\xi\rho A_v^3/2cl_v^2\sin^2\alpha)$.

Take a certain stroke (or crank angular velocity ω) of a reciprocating plunger pump as an example, if φ and ξ remain unchanged in equation (9). The description of the above symbols is shown in Table 1.

This article takes a typical BRW630/37.5 emulsion pump discharge valve as an example. Figure 4 represents a typical BRW630/37.5 emulsion pump. The structural parameters of the pump were stroke 0.07 m, plunger diameter 0.06 m, crank angular velocity 69.43 rad/s, medium density 1000 kg/m^3. The mass is 0.425 kg, the spring stiffness coefficient is 6.842 N/m, and the valve spring preload is 47.9 N.

We used Scilab software to perform simulation calculations. The spool of the pump valve was vibrated, and the displacement curve was slightly ridged. The spool opened when the crank angle was 25°. It reached the maximum value of 8.44 mm at 55°, then began to drop to 97°, and then began to rise again, until reaching the second peak point of 4.95 mm at 115.5°, mainly because of fluid lift, like the results of literature research. The spool closes when it drops to a crank angle of 180°, and there is no closing hysteresis.

4. Simulation Analysis of Emulsion Pump Based on AMESim

4.1. AMESim Model. The mechanical structure and motion state of the emulsion pump are relatively complicated, including the high-speed rotation of the motor, the low-speed and heavy-duty rotation of the crankshaft, and the excitation force generated by the reciprocating motion, as well as the reciprocation of the connecting rod-crosshead plunger mechanism. Figure 5 shows the schematic diagram of the spool displacement test system movement and nonlinear movement of the suction valve and the discharge valve. AMESim is a multidisciplinary complex system modeling and simulation platform. Many studies have used AMESim software to simulate and analyze emulsion pumps. We have used the AMESim software to model the hydraulic system of the emulsion pump. The model includes a crank connecting rod mechanism, suction valve, discharge valve, and other models. Table 2 presents the simulation parameters of the AMESim model.

4.2. Comparison and Analysis of Simulation and Test Results. This article adopted a monitoring system based on a linear variable differential transformer (LVDT) sensor, data acquisition system, and signal processing system to collect displacement data of pump valve spool. An LVDT sensor is generally used to convert mechanical motion or vibrations, specifically rectilinear motion, into a variable electrical current, voltage or electric signals, and the reverse. In the AMESim simulation results, the spool is closed at a crank angle of 203°, while the test results show that the spool closes at a crank angle of 308°. Figure 6 shows the U-Adolph simulation of displacement of the valve core, whereas

Table 1: Description of some symbols of emulsion pump.

Symbol	Meaning description
p_1	Liquid pressure acting under the valve disc
p_2	Liquid pressure acting on the valve disc
d_d	Centerline diameter of poppet valve disc
R_0	Spring preload
Q_g	Discharge volume in the cylinder
ϕ	Crank angle
$\xi = (1/u^2)$	μ is the flow coefficient of the valve
ρ	The density of working fluid
φ	Coefficient of force on the valve disc

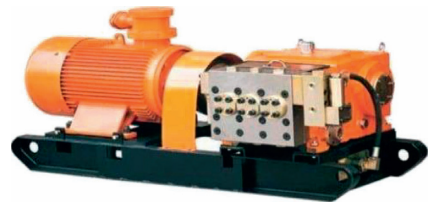

Figure 4: BRW630/37.5 emulsion pump.

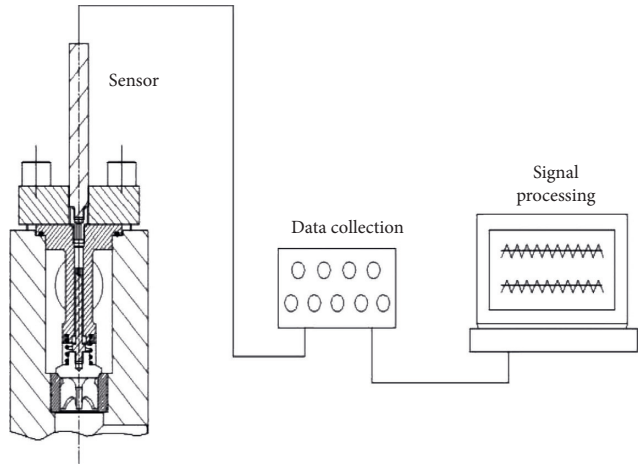

Figure 5: The schematic diagram of the testing system of displacement of pump valve.

Figure 7 shows the U-Adolph and AMESim simulation displacement of the valve core. The test medium used was pure water, the working frequency of the motor was 50 Hz, the pressure was controlled by the electromagnetic unloading valve with unloading pressure of 37.5 MPa, and the recovery pressure was 35 MPa. A test system based on LVDT sensors was used to collect and test valve core displacement data in a 37.5 MPa water medium.

Figures 8 and 9 show the comparison results of the spool displacement and opening speed of the two simulation methods. The AMESim simulation result assumes that the valve core opens when the crank angle is 25°. The maximum speed of valve core opening calculated by Adolf simulation was 2 m/s, while the result of AMESim simulation calculation was 0.5 m/s, and there was no spool vibration in the simulation results of AMESim. The Adolf displacement simulation result is 8.44 mm, while the AMESim simulation

Table 2: Simulation parameters for the AMESim model.

Model	Parameter	Numerical value
Crank connecting rod	Speed (r/min)	663
Suction/discharge valve	Crank radius (mm)	35
	Center distance of connecting rod (mm)	220
Orifice	Quality of suction valve (kg)	0.26
	Suction valve spring stiffness (N/mm)	3.8
	Suction valve spring preload (N)	38.5
	Diameter of suction valve (mm)	50.8
	Diameter of the upper rod of suction valve (mm)	22
	Effective flow diameter of suction valve (mm)	45
	Diameter of discharge valve (mm)	48
	Diameter of the upper rod of drain valve (mm)	22.4
	Effective flow diameter of discharge valve (mm)	40
Unloading valve	Unloading pressure	37.5

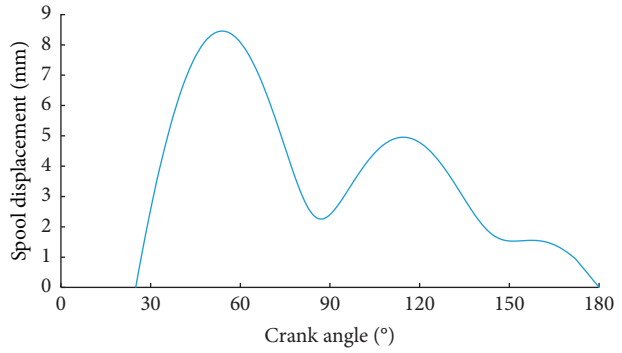

Figure 6: The U-Adolph simulation of displacement of the valve core.

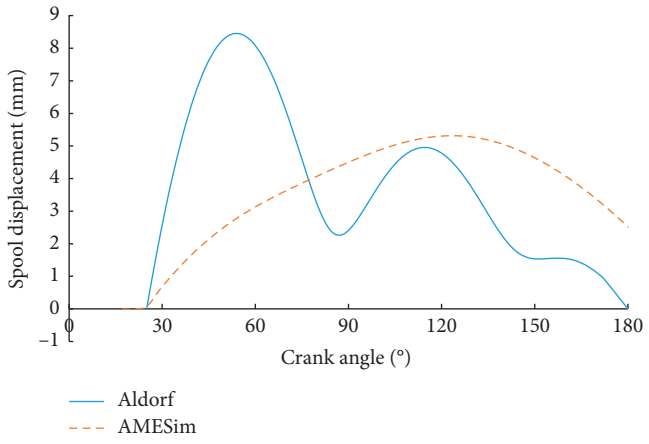

Figure 7: U-Adolph and AMESim simulation of the velocity of the valve core.

result is 5.29 mm, which shows a difference of 3.15% compared to the Adolf simulation result. Compared with Adolf's simulation results, the AMESim simulation result shows obvious spool closing hysteresis. The test result of the maximum displacement of the valve core is 8.27 speed/mm.

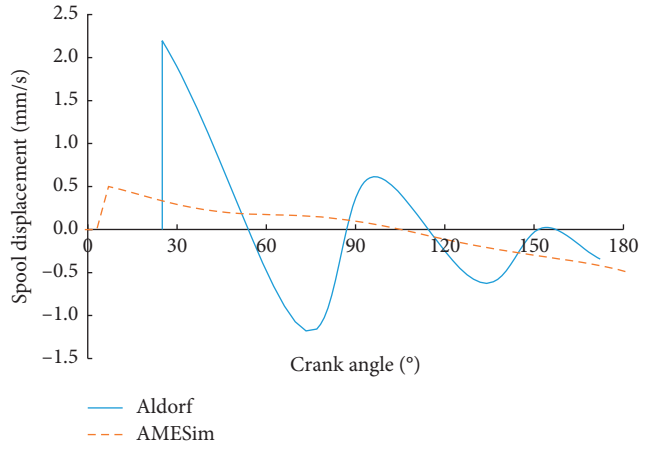

Figure 8: U-Adolph and AMESim simulation of displacement of the valve core.

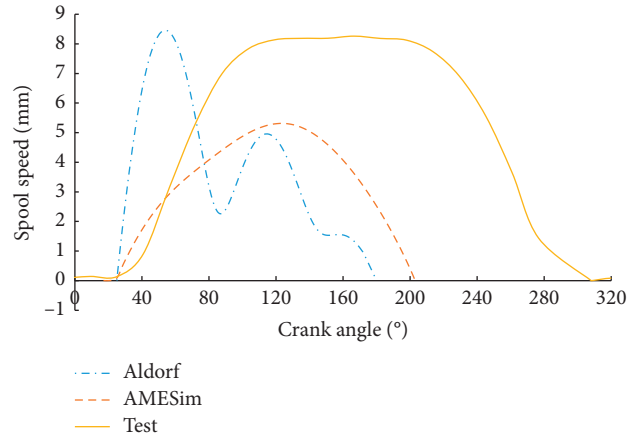

Figure 9: U-Adolph and AMESim simulation as well as test of displacement of the valve core.

4.3. Comparative Analysis of Simulation and Experiment. The phenomenon of spool vibration and the spool closing hysteresis verify the feasibility of using the simulation

method to study the movement characteristics of the pump and valve. The cost of testing and parameterized design is greatly reduced, which is helpful for the research and development of high reliability, high response, and high-efficiency emulsion pump valves. Both the spool displacement test results and the Adolf simulation method show chattering, but the test results show that the second wave crest phenomenon of Adolf simulation does not appear in the process of spool descent. Based on Scilab software, Adolf's precise differential equations are simulated and calculated to solve the spool movement characteristics of a BRW630/37.5 emulsion pump, and the spool displacement curve and spool movement speed curve are calculated. The calculation results show that the maximum displacement of the pump valve is 8.44 mm when the valve is opened, and vibration occurs during the closing process, and the displacement presents a subpeak value of 4.95 mm. In the AMESim simulation results, the spool closes at a crank angle of 203°, while the test results show that the spool closes at a crank angle of 308°. Therefore, the test result shows that the spool is closed at a crank angle of 308°. The closing hysteresis is even more pronounced. According to the results of Adolf's simulation, the spool opens at a crank angle of 25°, reaches a maximum value of 8.44 mm at 55°, and then drops. When it starts to rise to 115.5°, it reaches the second peak point of 4.95 mm, and then it is closed at 180°. Chattering occurs during the closing process and there is no closing hysteresis. The maximum speed of the spool opening is 2 m/s higher than the Adolf simulation result by 0.5 m/s. The test result of the maximum displacement of the spool is 8.27 mm. Compared with the test result, the Adolf simulation method is more accurate, and the deviation is only 2.1%, while the deviation of the AMESim simulation result is −36%. Compared with the test results, the Adolf simulation method simulates the vibration of the valve core during the closing process, but the second wave peak phenomenon in the simulation results does not appear in the test results, and the valve core vibration does not appear in the AMESim simulation results phenomenon. Both the test results and the AMESim simulation results show obvious spool closing hysteresis. The AMESim simulation results show that the spool closes at a crank angle of 203°, while the test result is 308°. Therefore, the spool closing hysteresis in the test results is more significant.

5. Conclusion

Studying the movement characteristics of the pump valve of the emulsion pump is of great significance for optimizing the dynamic response characteristics of the pump valve and improving the volumetric efficiency. We simulated Adolf's precise differential equations to solve the spool movement characteristics of a BRW630/37.5 emulsion pump, and the spool displacement curve and spool movement speed curve are calculated. The simulations results show that the maximum displacement of the pump valve is 8.44 mm when the valve is opened, vibration occurs during the closing process, and the displacement presents a subpeak value of 4.95 mm. The hydraulic system of the emulsion pump of the same model is simulated by AMESim software, and the displacement curve of the spool of the discharge valve and the speed curve of the spool movement is computed. The maximum opening speed and maximum displacement of the spool of AMESim are less than those of Adolf's simulation. There is no vibration during the opening and closing process of the discharge valve, and there is clear spool closing hysteresis. A test system based on LVDT sensors was used to collect and test valve core displacement data in a 37.5 MPa water medium. In terms of spool movement characteristics, the maximum displacement data deviation of the spool is only 2.1%, and spool vibration occurs in all cases. As compared to the AMESim simulation results, the test results have more significant spool closing hysteresis.

Data Availability

The data of this manuscript are all searchable on the Internet public channels.

Conflicts of Interest

The authors declare no conflicts of interest.

Acknowledgments

This study was supported by the National Key R&D Program Funded Project (2017YFC0804300 and 2017YFC0804304), China. This work was supported in part by Coal Science and Industry Group Science and Technology Innovation Fund Project (2018-TD-ZD015 and 2020-TD-ZD015), China.

References

[1] X. Wang, Y. J. Li, H. Yang, and Z. L. Xu, "Super-wetting, photoactive tio2 coating on amino-silane modified pan nanofiber membranes for high efficient oil-water emulsion separation application," *Journal of Membrane Science*, vol. 580, pp. 40–48, 2019.

[2] N. Kiama and C. Poncho, "Photoelectrocatalytic reactor improvement towards oil-in-water emulsion degradation," *Journal of Environmental Management*, vol. 279, 2021.

[3] J. Ruan, P. R. Ukrainetz, and R. Burton, "Frequency domain modelling and identification of 2D digital servo valve," *International Journal of Fluid Power*, vol. 1, no. 2, pp. 49–59, 2000.

[4] S. Liu, Q. Zhang, Q. L. Fan, and R. Wang, "3d superhydrophobic sponge coated with magnesium hydroxide for effective oil/water mixture and emulsion separation," *Industrial & Engineering Chemistry Research*, vol. 59, 2020.

[5] A. M. Sedlak, J. H. Yanta, and M. J. Lynch, "Intrathecal bupivacaine and morphine toxicity leading to transient hypotension and delayed status epilepticus," *American Journal of Emergency Medicine*, vol. 38, 2020.

[6] D. J. Berman, "A case of local anesthetic toxicity that wasn't: lipid rescue from self-administered benzodiazepine overdose in labor," *International Journal of Obstetric Anesthesia*, vol. 42, 2019.

[7] M. Omichi, Y. Ueki, and N. Seko, "Development of a simplified radiation-induced emulsion graft polymerization method and its application to the fabrication of a heavy metal adsorbent," *Polymers*, vol. 11, no. 8, 2019.

[8] P. Junfeng, H. Chao, and L. Miaorong, "The valve motion characteristics of a reciprocating pump," *Mechanical Systems and Signal Processing*, vol. 66-67, 2016.

[9] J. P. Leng, K. L. Xing, and P. P. Zhang, "Dynamic analysis of cartridge style pilot relief valves," *Applied Mechanics and Materials*, vol. 405–408, pp. 3279–3283, 2013.

[10] X. Lei and Y. Wu, "Simulation and result in an analysis of AMEsim for the relief valve dynamic characteristics experiment," in *Proceedings of the International Conference on Electrical and Control Engineering*, pp. 5587–5590, Wuhan, China, June 2010.

[11] K. Dasgupta and J. Watton, "Dynamic analysis of proportional solenoid controlled piloted relief valve by the bond graph," *Simulation Modelling Practice and Theory*, vol. 13, pp. 21–38, 2005.

[12] C. J. Sang and J. H. Kang, "Orifice design of a pilot-operated pressure relief valve," *Journal of Pressure Vessel Technology*, vol. 139, no. 3, 2017.

[13] C. Vallet, J. Ferrari, J. F. Rit et al., "Single-phase CFD inside a water safety valve," in *Proceedings of the ASME 2010 Pressure Vessels and Piping Division/K-PVP Conference*, pp. 335–342, Bellevue, WA, USA, July 2010.

[14] Q. H. Hao, W. R. Wu, X. J. Liang, and Z. Liu, "Effects of structure parameters on abnormal opening of pilot-operated relief valve under alternating pressure," *IEEE Access*, vol. 7, pp. 33932–33942, 2019.

[15] C. Tian and X. Wei∗, Y. Zheng, The intelligent control of emulsion pump station," in *Proceedings of the 2nd International Conference on Computing and Data Science (CONF-cds 2021)*, vol. 1881, New York; NY, USA, June 2021.

[16] L. Xiu and W. Yajun, "Simulation and result analysis of AMEsim for the relief valve dynamic characteristics experiment," in *Proceedings of the 2010 International Conference on Electrical and Control Engineering*, Wuhan, China, June 2010.

[17] G. Yongjun, W. Zuwen, X. Jie, and Z. Zengmeng, "Simulation and experiments study on water hydraulic pressure relief valve with pilot stage," *Journal of Mechanical Engineering*, vol. 46, no. 24, pp. 136–142, 2010.

[18] M. Xuyao, L. Bin, L. Yiou, H. Junhua, and L. Qiwei, "Design & simulation of a hydraulic back pressure valve with a large flow range," *Journal of Physics: Conference Series*, vol. 1213, no. 4, 2019.

[19] J. Ruan, P. R. Ukrainetz, and R. Burton, "Frequency-domain modeling and identification of 2D digital servo valve," *International Journal of Fluid Power*, vol. 1, pp. 49–59, 2000.

[20] M. Georgy, "Fatigue failure mechanisms of the pressure relief valve," *Journal of Loss Prevention in the Process Industries*, vol. 48, pp. 1–13, 2017.

[21] E. Lisowski and G. Filo, "Analysis of a proportional control valve flow coefficient with the usage of a CFD method," *Flow Measurement and Instrumentation*, vol. 53, pp. 269–278, 2017.

[22] V. Sverbilov, D. Stadnick, and G. Makaryants, "Study ondynamic behavior of a gas pressure relief valve for a big flow rate," in *Proceedings of the ASME/BATH 2013 Symposium on Fluid Power and Motion Control*, Sarasota, FL, USA, October 2013.

[23] S. Hua, K. Han, and Z. Xu, "Image processing technology based on internet of things in intelligent pig breeding," *Mathematical Problems in Engineering*, vol. 2021, Article ID 5583355, 9 pages, 2021.

[24] Q. Tie and Z. Zhao, "Underwater internet of things in the smart ocean: system architecture and open issues," *IEEE Transactions on Industrial Informatics*, vol. 16, 2020.

[25] B. Vha, B. Gtce, C. Lap, and D. Ogb, "Internet of things in arable farming: implementation, applications, challenges and potential-ScienceDirect," *Biosystems Engineering*, vol. 191, pp. 60–84, 2020.

[26] J. Chauhan and P. Goswami, "An integrated metaheuristic technique based energy-aware clustering protocol for internet of things based smart classroom," *Modern Physics Letters*, vol. 34, 2020.

[27] W. Chen, J. Niu, I. Liu, C. Chi, and W. Liu, "Study of a palladium (pd)/aluminum-doped zinc oxide (azo) hydrogen sensor and the Kalman algorithm for internet-of-things (IoT) application," *IEEE Transactions on Electron Devices*, vol. 67, no. 10, pp. 4405–4412, 2020.

[28] G. Goswami and P. K. Goswami, "Self-adaptive learning based controller to mitigate pq issues in the internet of things devices," *International Transactions on Electrical Energy Systems*, vol. 31, 2021.

[29] P. Kumar and L. Chouhan, "Design of secure session key using unique addressing and identification scheme for smart home internet of things network," *Transactions on Emerging Telecommunications Technologies*, vol. 10, p. e3993, 2020.

[30] D. Bi, S. Kadry, and P. Kumar, "Internet of things assisted public security management platform for urban transportation using hybridized cryptographic-integrated steganography," *IET Intelligent Transport Systems*, vol. 14, 2020.

[31] H. Pajooh, M. Rashid, M. F Alam, and S. Demidenko, "Multi-layer blockchain-based security architecture for the internet of things," *Sensors*, vol. 21, no. 3, p. 772, 2020.

[32] M. Yu, T. Quan, Q. Peng, X. Yu, and L. Liu, "A model-based collaborate filtering algorithm based on stacked AutoEncoder," *Neural Computing, and Applications*, vol. 11, no. 7, pp. 231–244, 2021.

[33] X. Yu, F. Jiang, and J. Du, "A cross-domain collaborative filtering algorithm with expanding user and item features via the latent factor space of auxiliary domains," *Pattern Recognition*, vol. 94, pp. 96–109, 2019.

[34] G. Mu, F. Wang, X. Mi, and G. Gao, "Dynamic modeling and analysis of compressor reed valve based on movement characteristics," *Applied Thermal Engineering*, vol. 150, pp. 522–531, 2019.